

Simultaneous Enhancement in Strength and Toughness of Composites of poly(lactic acid)/ poly (butylene adipate-co-terephthalate)/ nano-sized Calcium Carbonate by UV Irradiation

Zhenyu Guo¹, Weiqiang Song^{1*}, Xiaowen Long¹, Yuqi Song¹, Xueqin Wei¹, Wenxi Cheng¹, Yu Feng², Yihong Song³, Xingchu He⁴ and Hongsen Wang⁴

¹School of Materials Science and Engineering, Henan University of Technology, Zhengzhou 450001, China

²School of Art, Henan University of Technology, Zhengzhou 450001, China

³School of Art and Design, Zhengzhou University of Aeronautics, Zhengzhou 450046, China

⁴Henan Hairuixiang Technology Co., Ltd, Pingdingshan 467100, China

*Corresponding Author: Weiqiang Song, School of Materials Science and Engineering, Henan University of Technology, Zhengzhou 450001, China, Tel.: +8618623719057, E-mail: weiqiang_song@haut.edu.cn

Citation: Zhenyu Guo, Weiqiang Song, Xiaowen Long, Yuqi Song, Xueqin Wei et al. (2023) Simultaneous Enhancement in Strength and Toughness of Composites of poly(lactic acid)/poly(butylene adipate-co-terephthalate)/nano-sized Calcium Carbonate by UV Irradiation. Chem Eng Sci. 1: 1-16

Copyright: © 2023 Zhenyu Guo. This is an open-access article distributed under the terms of Creative Commons Attribution License, which permits unrestricted use, distribution, and reproduction in any medium, provided the original author and source are credited.

Abstract

Series of composites of poly(lactic acid) (PLA) and poly(butylene adipate-co-terephthalate) (PBAT) with constant amounts of calcium carbonate, benzophenone and triallyl isocyanurate were prepared by using a double screw extruder, and blown into films by extrusion blow molding. After UV exposure with irradiation doses (ID) of 20 J/cm² and 40 J/cm², the mechanical, dynamic mechanical and thermal properties were investigated by comparing them with the un-irradiated films. The results showed that UV irradiation increased the tensile strength and decrease the fracture energy of PLA/PBAT (100/0), simultaneously increased the tensile strength and fracture energy of PLA/PBAT (70/30), but simultaneously decrease the tensile strength and fracture energy of PLA/PBAT (50/50). The glass transition temperature (T_g) of PLA/PBAT (100/0) increased after UV exposure, but the T_g of PLA/PBAT (70/30) and (50/50) unchanged or varied within the error range. The crystallization temperature (T_c) did not changed after UV exposure, but the crystallizability significantly decreased. The difference was attributed to the PLA/PBAT ratios. UV irradiation was revealed to be a simple and effective technique to simultaneously improve the strength and toughness of LA/PBAT films with bicontinuous phases.

Keywords: UV irradiation; poly (lactic acid); poly (butylene adipate-co-terephthalate); nano-sized calcium carbonate; simultaneous enhancement

Introduction

Poly(lactic acid) (PLA) is a polyester linear polymer from renewable resources with good bio-compatibility and complete biodegradability. It has become a hot research topic today due to its mechanical strength and properties similar to those of general polymeric materials [1-3]. As the most promising green plastic, its films, sheets and fibers have been widely used in textile [4]. Packaging [5], agriculture [6], health care [7], daily necessities [8] and other fields [9]. Nevertheless, its use is still restricted due to its hardness and brittleness, low processability and heat resistance [10-13]. Therefore, the modification of PLA is also required [14-17]. Up to now, a large number of studies have shown that the mechanical and thermal properties were improved when PLA chains were cross-linked to a certain degree, owing to that the movement of the chains in the amorphous region was sufficiently restrained even at a temperature higher than T_g .

The crosslinking method imparted a network structure to PLA while retaining its biodegradability, and adjusting its degradation cycle by controlling the reaction conditions and process parameters. Crosslinking of PLA mainly refers to the reaction of monomers with PLA in presence of cross-linking agent or ionizing radiation to form a crosslinking structure. The method mainly included chemical crosslinking [18-21], molecular modification crosslinking [22-26] and ionizing radiation crosslinking [27-32]. Cross-linking agent and initiator were usually used in the chemical method to initiate PLA chains to form cross-linking structure, and the effect of chemical cross-linking on PLA was greatly affected by the type of cross-linking agent, process parameters and other factors. The so-called molecular modification crosslinking was a method implemented by modifying the terminal groups of PLA chains to form active sites such as terminal double bonds. In this method, crosslinking structures were formed by initiating the polymerization of the chains with active terminal groups by a free radical polymerization mechanism. Actually, both chemical crosslinking and molecular modification crosslinking belonged to chemical methods. However, the chemical methods were so complicated, which undoubtedly increased the material cost and reduced the competitiveness of PLA products in the market. In contrast, ionizing radiation crosslinking is a typical "3E" technology, that is, efficient, environment-friendly and energy-saving. The irradiation crosslinking of PLA was realized by using γ ray and electron beam. Compared with chemical methods, irradiation crosslinking not only had fast reaction rate and high yield, but also avoided the problems of energy waste and the solvent recovery in chemical crosslinking. Nevertheless, the ionizing radiation caused crosslinking of PLA materials may still lack in the practical applicability considering cost of the equipment. Therefore, the crosslinking of PLA materials, whether by chemical methods or ionizing radiation methods, has shortcomings. Ultraviolet (UV) radiation is a promising alternative.

Although the ultraviolet light (UV) is not as powerful as ionizing radiation in terms of penetration, its penetration rate for thin films is still very high. In fact, UV crosslinking of polymer films has become increasingly popular due to continuous and environmentally-friendly process, cost and space saving, as well as cost-effectiveness. With the widespread use of PLA films, the use of UV radiation for PLA modification appears to be urgent. Further, fully biodegradable plastic bags in supermarkets are mainly a composite of PLA with poly (butylenedipate-co-terephthalate) (PBAT) and calcium carbonate (CaCO_3), but need to be improved in terms of toughness and strength to meet the diversity of applications. In the practical applications, the film strength plays an important role in mechanical paving or handling, which ensures the film integrity and usability. In the present study, the aim was to improve the mechanical properties of the PLA/PBAT/ CaCO_3 film by using UV radiation, and to propose a low-cost biodegradable films with good mechanical performance.

On the other hand, the morphology of PLA/PBAT blends changes with the ratio of PLA and PBAT. Li et al. [33] observed three different morphologies in PLA/PBAT blends, namely spherical droplets, elongated fibrous structures and co-continuous structures, as the PBAT content increased from 5 wt% to 50 wt%. Deng et al. [34] gave morphological maps of PLA/PBAT blends in the full component range as inferred from melt viscosity, optical micrographs, tensile properties and SEM fracture surfaces. When the content was below 5.0%, PBAT was dissolved in the PLA phase. Above 5.0%, PBAT separated from the PLA phase and forms droplets, which were uniformly dispersed in the continuous PLA phase. The structure formed was the so-called "island" morphology.

In the composition range of 19.0 to 40 wt%, PBAT and PLA formed a co-continuous phase. Above 40 wt%, PBAT formed a continuous phase and PLA became a dispersed phase. In this study, the PLA/PBAT/CaCO₃ films with PLA/PBAT ratios of 100/0, 70/30 and 50/50 in the presence of benzophenone (BP) and triallyl isocyanurate (TAIC) were radiated by UV light, and the effect of UV radiation and the continuous phase on the properties of the films was comparatively investigated.

Experimental

Materials: PLA (FY801, density: 1.24 g cm⁻³, MFR=4 g/10 min at 190°C and 2.16 kg) was purchased from Anhui Fengyuan Co. PBAT (blow molding grade) was purchased from Lanshan Tunhe Co. Nano-sized calcium carbonate (nano-CaCO₃, ≥ 98.5%, D50 65nm, stearic acid as activating agent) were supplied by Nanzhao Dingcheng Calcium Industry Co. Glycerol methacrylate (GMA), benzophenone (BP) and triallyl isocyanurate (TAIC) were analytically pure and purchased from Shanghai Aladdin Bio-chemical Technology Co., Ltd. Chemical structures of PLA, PBAT, GMA, TAIC, and BP are shown in Figure 1.

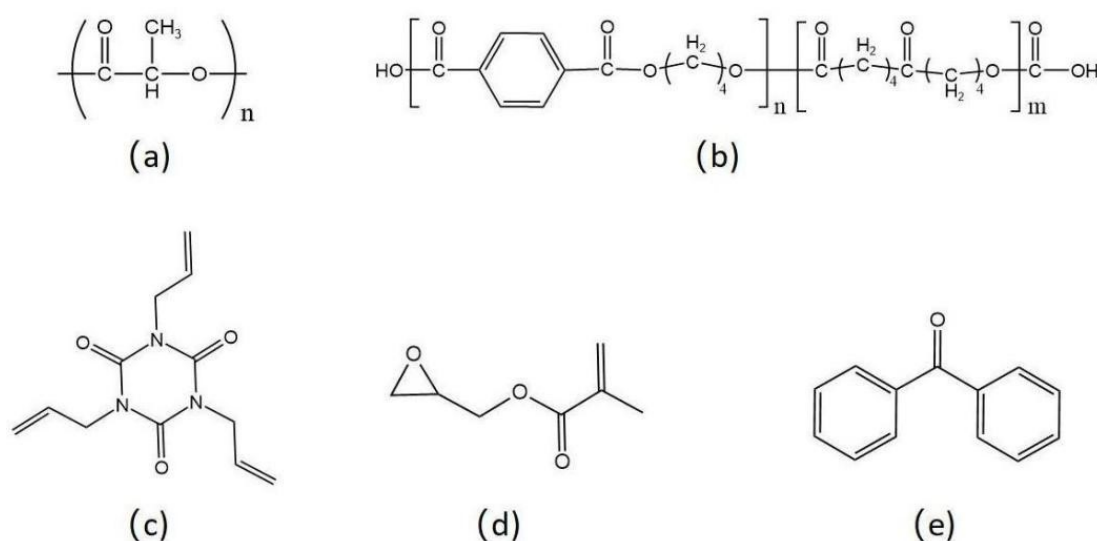


Figure 1: Chemical structures of (a) PLA, (b) PBAT, (c) TAIC, (d) GMA and (e) BP

Preparation of PLA/PBAT films: Both PLA and PBAT pellets were dried under vacuum at 80 °C for 3 hours to minimize the moisture. The components in PLA/PBAT composites were listed in Table 1.

Table 1: Feed ratio and irradiation dose of PLA/PBAT films

| | PLA | PBAT | GMA | TAIC | BP | CaCO ₃ | ID (J/cm ²) |
|--------------|-----|------|-----|------|-----|-------------------|-------------------------|
| PLA100 | 100 | 0 | 2 | 1.5 | 0.5 | 3 | 0 |
| PLA100/ID20 | 100 | 0 | 2 | 1.5 | 0.5 | 3 | 20 |
| PLA100/ID200 | 100 | 0 | 2 | 1.5 | 0.5 | 3 | 40 |
| PLA70 | 70 | 30 | 2 | 1.5 | 0.5 | 3 | 0 |
| PLA70/ID20 | 70 | 30 | 2 | 1.5 | 0.5 | 3 | 2 |
| PLA70/ID200 | 70 | 30 | 2 | 1.5 | 0.5 | 3 | 40 |
| PLA50 | 50 | 50 | 2 | 1.5 | 0.5 | 3 | 0 |
| PLA50/ID20 | 50 | 50 | 2 | 1.5 | 0.5 | 3 | 20 |
| PLA50/ID200 | 50 | 50 | 2 | 1.5 | 0.5 | 3 | 40 |

The PLA/PBAT composites were prepared in a twin-screw extruder at a screw speed of 60 rpm and temperatures set at 170 °C to 180 °C from the feed zone to die. The PLA/PBAT films were prepared by using a blown-film extrusion process.

UV irradiation: A UV light curing machine was used. The irradiation was carried out on one side of the films laid flat on a conveyor belt, and the UV irradiation dose (ID) was controlled by the running speed of the conveyor belt at the room temperature. ID was set at 20 J/cm^2 and 40 J/cm^2 . The vertical distance between the conveyor belt and the UV light source was fixed at 15 cm. The radiation process is shown in Figure 2.

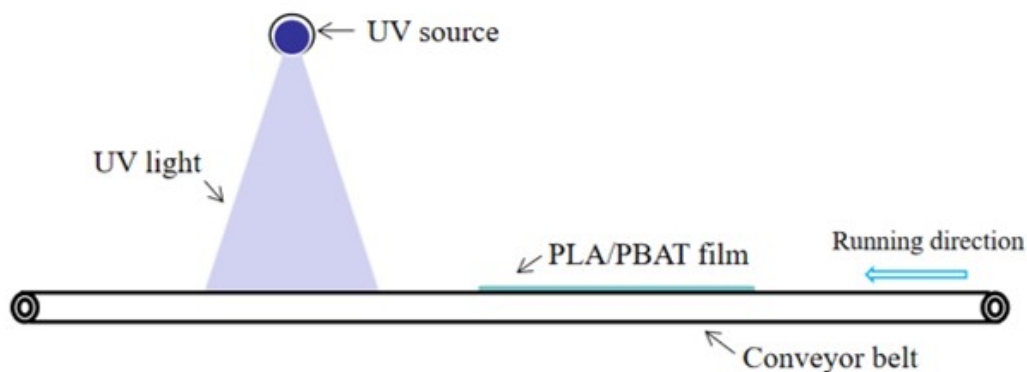


Figure 2: Radiation process by using UV light

Material Characterization. Tensile Testing The tensile testing was performed using a film tensile tester (WDW-100NE, Jinan Chuanbai Instrument Equipment Co., Ltd, China), equipped with a 100 N load cell. Rectangular samples of 25-mm wide and 100-mm long were cut from the blown-film samples. The test was conducted at a cross-head speed of 5 mm/min and gauge length of 50 mm. All reported results were the averages of at least five test specimens.

Dynamic Mechanical Analysis (DMA). The relaxation of amorphous molecular chains was measured by dynamic mechanical analysis (DMA Q800, TA instruments, USA) in frequency-strain scanning mode with a preload force of 0.01 N. The rectangle sample with a thickness of $60 \pm 3 \mu\text{m}$ and a width of 8 mm was tested from $25 \text{ }^\circ\text{C}$ to $120 \text{ }^\circ\text{C}$ at the heating rate of $5 \text{ }^\circ\text{C}/\text{min}$. The frequency and amplitude were fixed at 1 Hz and $10 \mu\text{m}$, respectively.

Differential Scanning Calorimetry (DSC). Thermal transitions of PLA/PBAT films were investigated using a differential scanning calorimeter (DSC) (DSC 200 F3, Netzsch Scientific Instrument Co., Ltd, China). The samples ($19 \pm 1 \text{ mg}$) on DSC testing were obtained from the corresponding films. The samples were heated to $250 \text{ }^\circ\text{C}$ in a nitrogen atmosphere and held for 5 min to eliminate thermal history, and then cooled to the room temperature. Afterwards, the samples were reheated to $250 \text{ }^\circ\text{C}$. The heating and cooling rates were both set at $20 \text{ }^\circ\text{C}/\text{min}$.

Ultraviolet Visible Spectrum. A L5S UV-visible spectrophotometer was used to study the optical properties of the prepared films by recording the percent transmission spectra in the ultraviolet and visible range. Prepared films were cut into a square of 50 mm size and loaded in the spectrophotometer cell and transmittance spectra were recorded with respect to air.

FTIR measurements. Measurement of the Fourier Transform Infra Red (FTIR) spectroscopy was carried out using the Thermo Scientific Nicolet iS5 FTIR spectrometer. The transmission of the infrared spectra was obtained in the range between 400 cm^{-1} to 4000 cm^{-1} at a 4 cm^{-1} spectral resolution by attenuated total reflection (ATR) mode, and 64 scans were added. The ATR element used was made of type II diamond (refractive index is 2.42) with the incident angle of 45° . The difference between the FTIR spectra was studied to find any new form of bond or interaction.

Results and Discussion

Tensile Property Results. Figure 3A-C shows the stress-strain curves of the non-irradiated and irradiated films with PLA/PBAT ratio of 100/0, 70/30 and 50/50. Figure 3D shows tensile modulus and yield stress based on the stress-strain curves. Irradiation at 20 J/cm² increased tensile modulus and yield stress of PLA100 by 18% and 33%, respectively, while irradiation at the same dose increased that of PLA70 by 21% and 13%. But the irradiation had no effect on the that of PLA50. This likely indicates that UV irradiation imparting stiffness enhancement depends on the PLA/PBAT ratio in the films. Compared with that of PLA100, further irradiation at 40 J/cm² continued to increase tensile modulus and yield stress of PLA100/ID200 by 24% and 17%, respectively, and increase that of PLA70 31% and 25%, respectively. It should be noted that yield stress of PLA100/ID20 declined by 13% compared to that with ID 20 J/cm².

In addition, further irradiation had almost no effect on tensile modulus and yield stress of PLA50. This indicates that UV irradiation is beneficial for improving tensile modulus and yield stress of PLA70. Figure 3E shows elongation at break and fracture energy of the films. Elongation at break and fracture energy of PLA100 kept decreasing significantly with the increase of ID, while that of PLA50 decreased by 10% and 18%, respectively. In addition, elongation at break and fracture energy of PLA70 increased and then decreased with ID. The above results suggest that elongation at break and fracture energy of PLA70 can reach their maximum at a certain ID.

To improve the suitability of poly(lactic acid) (PLA) for implantable devices, it ideally needs greater ductility without losses in strength. Zhao et al. [35] utilized UV irradiation as a bulk modification method to increase the long-term stability of PLA with poly(2-ethyl-2-oxazoline) (PEtOx). The PLA blend showed improved tensile strength and elongation-at-break with small amounts of PEtOx added (1.5 wt%).

Crosslinking by UV irradiation showed significant improvements with dibutyltin dilaurate as a catalyst and was only possible with the added PEtOx present. In the current study, fracture energy of PLA70/ID20 was improved with increase in tensile modulus and yield stress in the presence of 0.5 parts BP as photoinitiator and 1.5 parts TAIC as crosslinking agent.

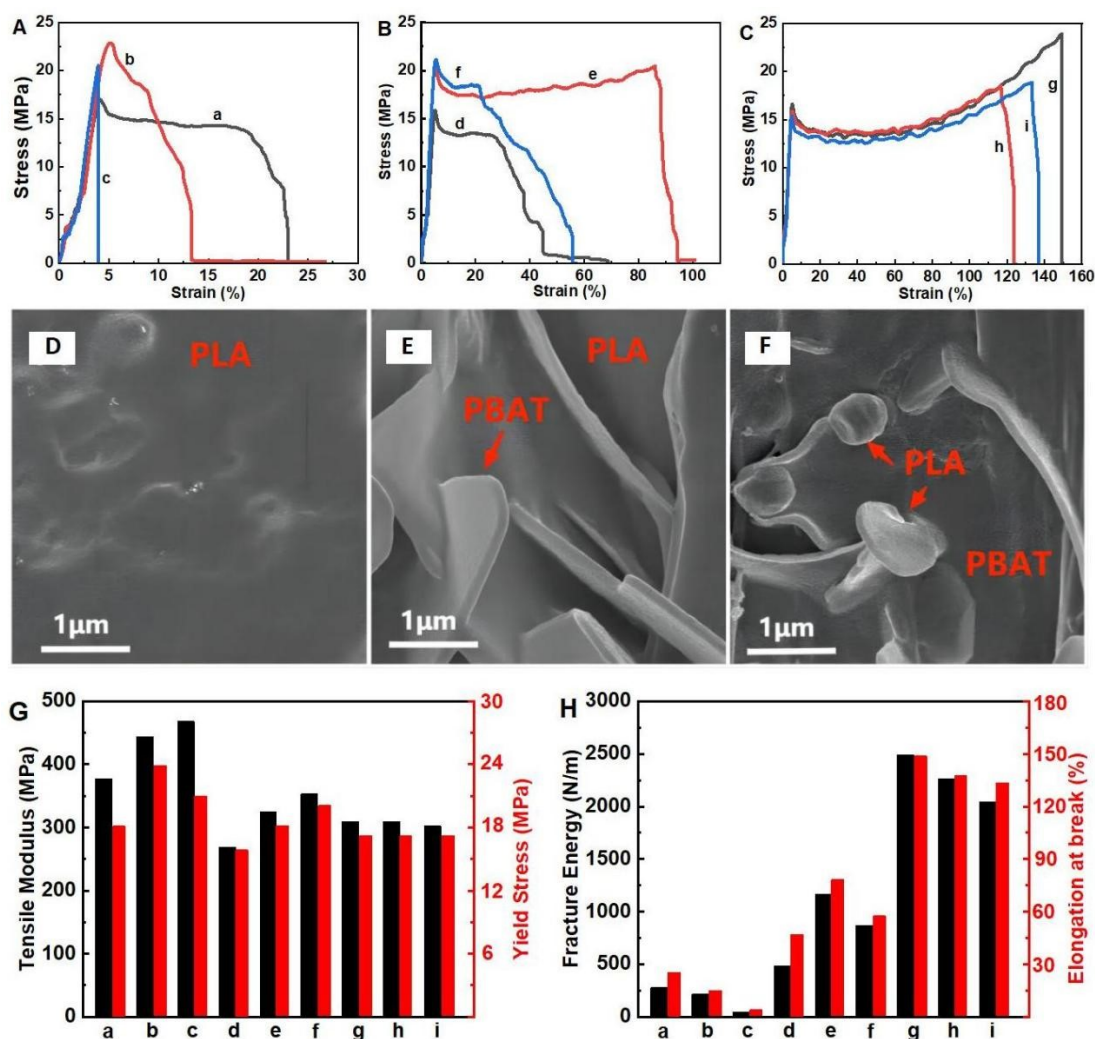


Figure 3: Stress-strain curves of (A) PLA100, (B) PLA70 and (C) PLA50 before and after UV exposure. SEM images of fracture surfaces of (D) PLA100, (E) PLA70 and (F) PLA50. (G) Tensile modulus and yield stress, and (H) fracture energy and elongation at break before and after UV exposure: (a) PLA100, (b) PLA100/ID20, (c) PLA100/ID40, (d) PLA70, (e) PLA70/ID20, (f) PLA70/ID40, (g) PLA50, (h) PLA50/ID20 and (i) PLA50/ID40

SEM Results: The difference in the tensile behavior of the irradiated PLA/PBAT films likely stems from the morphology of the composites. Figure 3D-F shows the SEM micrographs of the fracture cross-section of the composite in the impact test. The micrographs provide interesting information on the blend morphology and highlight the difference of the continuous phase as a function of the PLA content. While PLA100 exhibits a relatively smooth fracture surface with its expected brittle behavior, PLA70 displays a rough fracture surface with lamellar PBAT phase distributing in a continuous phase of PLA. In PLA50, PLA is present as spheroidal domains distributed in the PLA matrix. Many articles [13] inferred the relationship between the morphology and composition of PLA/PBAT blends in more detail from various analyses such as melt viscosity, optical micrographs, tensile behavior, and SEM fracture surface. With the increase of PBAT content from 5 wt % to 50wt %, PBAT as the dispersed phase gradually transitions from a spherical droplet, elongated fiber structure to a co-continuous structure with PLA. When the content exceeded 70 wt %, PLA transformed into the dispersed phase [28]. The morphology with PLA/PBAT bi-continuous phases in PLA70 facilitated the formation of a larger contact area, which promoted compatibility between PLA and PBAT. On the other hand, UV irradiation caused both cross-linking and degradation. When TAIC was used, the cross-linking prevailed with respect to the degradation, which enhanced the compatibility of PLA and PBAT phases more effectively. The large contact area and the more effective cross-linking on the interface improved both strength and toughness of PLA70.

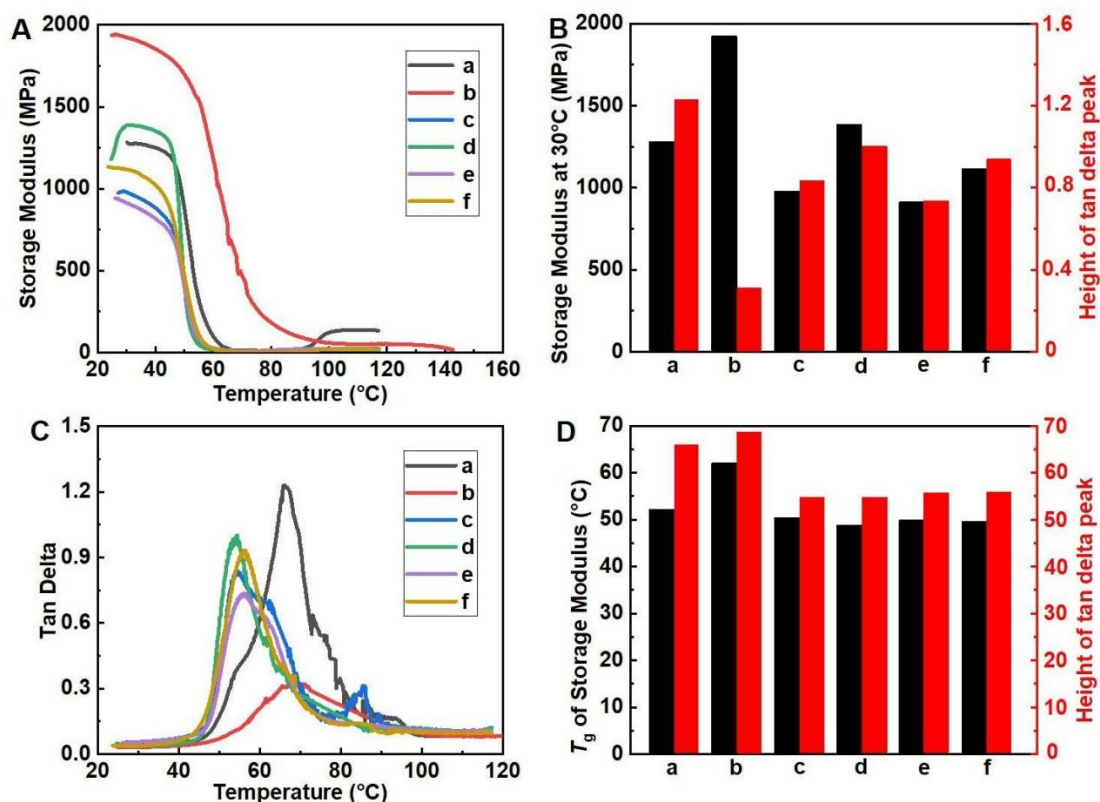


Figure 4: DMA analysis of (A) temperature dependence of storage modulus, (B) storage modulus obtained at 30 °C and tan δ peak intensity, (C) temperature dependence of tan δ , (D) T_g (E), and T_g (tan δ): (a) PLA100, (b) PLA100/ID20, (c) PLA70, (d) PLA70/ID20, (e) PLA50, and (f) PLA50/ID20

DMA Results. Figure 4A-D shows the measured temperature dependence of the storage modulus and tan δ of the PLA-based films. The storage moduli (obtained at 30 °C) of PLA100/ID20, PLA70/ID20 and PLA50/ID20 were 50%, 44%, and 22% higher than those of the unirradiated films. This indicates an increase in the stiffness, which is consistent with the reinforcing effect of UV irradiation and measured tensile moduli. UV irradiation might cause the crosslinking structure of PLA under UV irradiation. Generally, crosslinking and chain scission proceed simultaneously in the presence of high UV radiation energy. But crosslinking structure can be effectively introduced into poly(lactic acid) (PLA) by UV irradiation with the presence of a small amount of benzophenone (BP) [36]. The resulted crosslinking structure increased the storage moduli of the radiated films. In addition, the intensity of the tan δ peak of PLA100/ID20 was 75% lower than that of PLA100, which indicates that the segmental chain motion of PLA was stunted by the crosslinking structure of PLA caused by UV irradiation in PLA100/ID20. But, the intensity of the tan δ peaks of PLA70/ID20 and PLA50/ID20 were 19% and 27% higher than that of PLA70 and PLA50, respectively, which suggested a freer motion of PLA chains in PLA70/ID20 and PLA50/ID20 films.

After UV exposure at 20 J/cm², the T_g (E) and T_g (tan δ) of PLA100/ID20 were, respectively, 19% and 5% higher than those of PLA100, which suggests low flexibility of PLA chains in PLA100/ID20. The crosslinking structure caused by UV irradiation might limit the PLA chain mobility, which resulted in an increase of T_g for the irradiated PLA100/ID20 film.

DSC Results. Figure 5A shows DSC first-cool-flow curves for the films. The exothermic peak temperatures of crystallization are listed in Figure 5B. When cooling down from the molten state, PLA100 and PLA100/ID20 went through dual crystallization. The crystallization at about 142 °C was attributed to the formation of perfect PLA grains, and that at about 114 °C to the formation of imperfect PLA grains. The crystallization at about 142 °C in PLA70, PLA50 and their irradiated counterparts is observed, but the exothermic peak at about 114 °C is very flat or almost invisible. The disappearance of the exothermic peak at about 114 °C might be consistent with the low content of PLA in PLA70 and PLA50. The almost identical crystallization temperature before and after irradiation indicates that UV irradiation had little effect on the crystallization behavior of PLA in the PLA-based films.

Figure 5C shows DSC second-heat-flow curves for PLA-based films. The cold crystallization temperature (T_{cc}) and melting temperature (T_m) are listed in Figure 5D. All unirradiated films, involving PLA100, PLA70 and PLA50, showed significant dual cold crystallization at about 110 °C and 146 °C. The occurrence of cold crystallization indicates that the PLA crystallization rate in the unirradiated films did not catch up with the cooling rate of -20 °C/min during the cooling cycle. However, all irradiated films, including PLA100/ID20, PLA70/ID20, and PLA50/ID20, did not exhibit cold crystallization. And, the heat of fusion were also particularly small, which indicated a very low crystallinity. Similarly, Koo et al. [36] effectively introduced crosslinking structure into poly(lactic acid) (PLA) by UV irradiation in the presence of 3.6% BP. The crosslinking lowered or even depressed both the melting point and cold crystallization enthalpy of the irradiated PLA samples. The photo-crosslinking of PLA was attributed to the recombination of primary and tertiary carbon radicals in the repeating units which were generated by the hydrogen abstraction of BP. With increasing crosslinking, melting peak disappeared and glass transition temperature elevated with loss of crystallinity, indicating that the crosslinking occurred in the crystalline region as well as in the amorphous region.

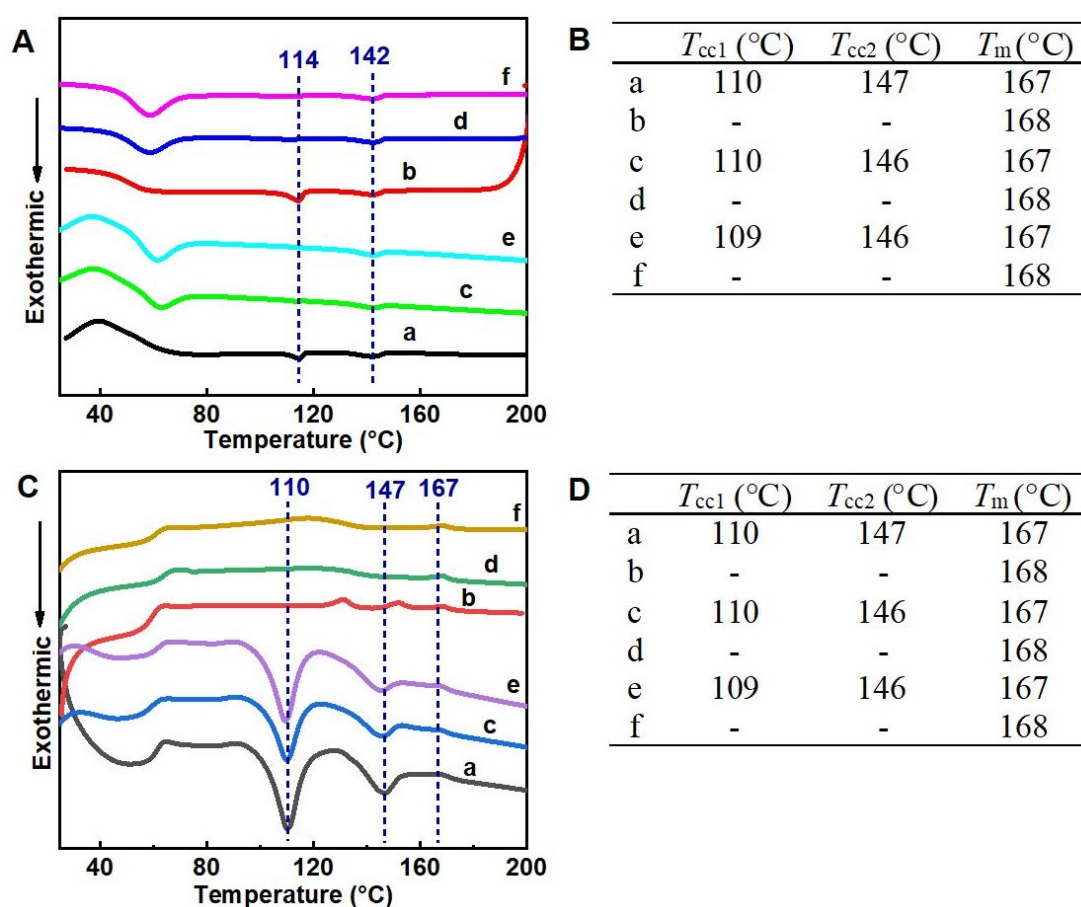


Figure 5: (A) DSC second-cool-flow curves, (B) Crystallization temperature in low and high temperature regions (T_{cc1} and T_{cc2}). (C) DSC second-heat-flow curves, (D) Cold crystallization temperature (T_{cc1} and T_{cc2}) and melting temperature (T_m): (a) PLA100, (b) PLA100/ID20, (c) PLA70, (d) PLA70/ID20, (e) PLA50, and (f) PLA50/ID20.

FTIR Results. Figure 6A-D shows the FTIR spectra of the PLA-based films and radiated films. All the films exhibited peaks of C-H stretching (around 2995 cm^{-1}), C=O stretching (around 1759 cm^{-1}), C-H bending (around 1455 cm^{-1}), C-O stretching (around 1185 and 1095 cm^{-1}), and C-C stretching (around 868 cm^{-1}). These peaks are consistent with the previously reported FTIR results in the literature. With the addition of PBAT, no obvious new peaks were observed in PLA70 and PLA50, but the peaks of C-H stretching (2900-3030 cm^{-1}) became stronger and broader, which are attributed to the benzene ring in the main chains of PBAT.

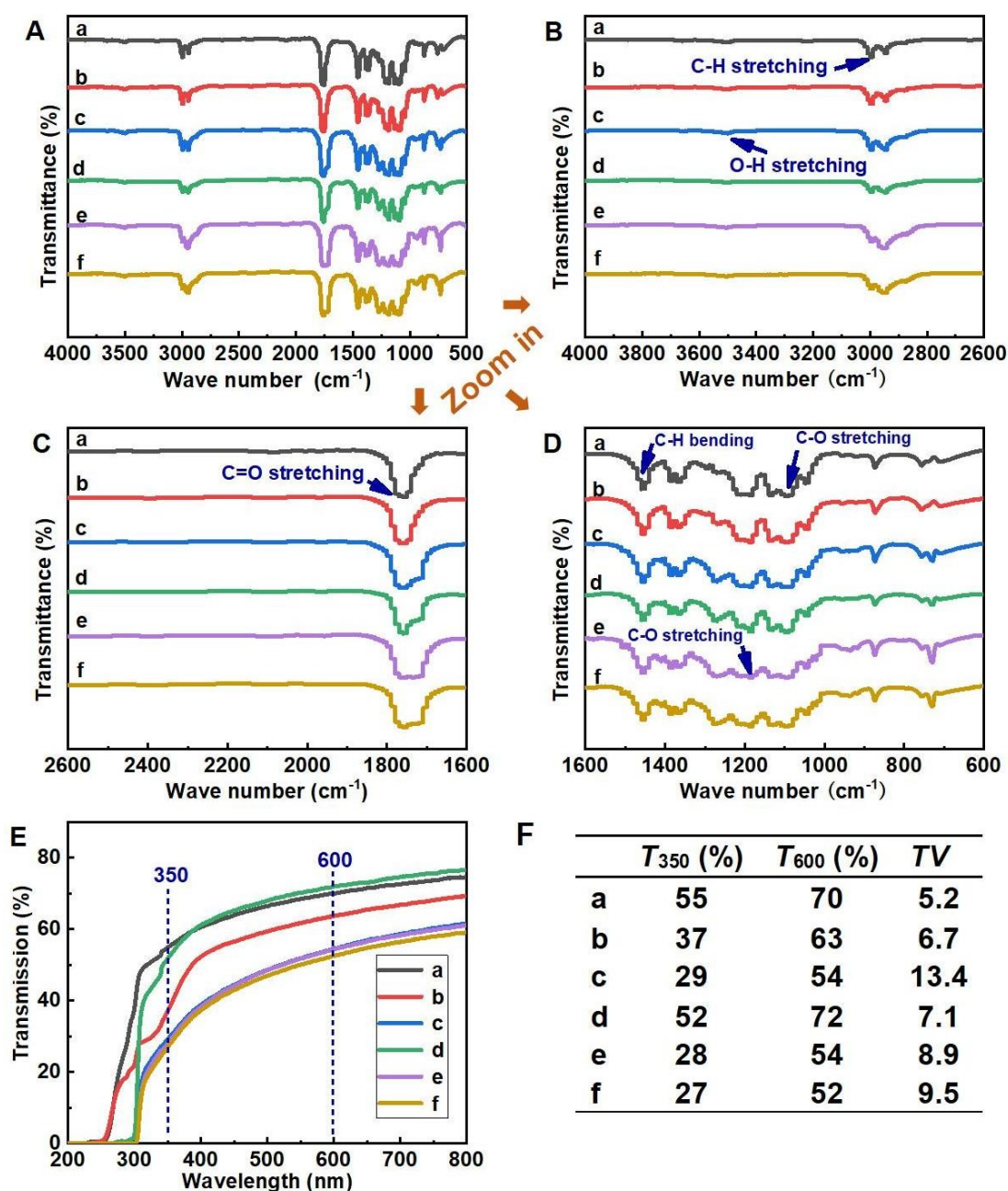


Figure 6: (A) FTIR curves (4000-500 cm⁻¹), (B) FTIR curves (4000-2600 cm⁻¹), (C) FTIR curves (2600-1600 cm⁻¹), (D) FTIR curves (1600-600 cm⁻¹), (E) UV-Visible spectra, and (F) ultraviolet analysis of (a) PLA100, (b) PLA100/ID20, (c) PLA70, (d) PLA70/ID20, (e) PLA50, and (f) PLA50/ID20.

Optical Properties. The optical properties of PLA/PBAT/CaCO₃ films were studied by recording percentage transmission spectra in UV-visible range (200-800 nm wavelength). Transmission spectra of the prepared films are illustrated in Figure 6E and the corresponding values along with transparency value (TV) are reported in Figure 6F. Transparency value of the films were computed with the help of following equation:

where T_{600} is the fractional equivalent of percentage transmission of 600 nm wavelength radiation and x is the film thickness in mm. A lower value of TV indicates higher transparency. The lowest value of TV corresponding to PLA100 film indicates highest transparency among the films, and the highest value of TV corresponding to PLA70 film indicates lowest transparency. After UV exposure, the transparency of PLA100/ID20 and PLA50/ID20 declined, but that of PLA70/ID20 rose.

PLA100 transmitted 55% and 70% of incident radiation in UV and visible range, but decreased to 37% and 63% after UV exposure, respectively. Similarly, the transmittance of PLA50 in UV and visible range decreased after UV exposure, although to a small extent. Differently, the light transmission of PLA70/ID20 was elevated compared to that of PLA70. This reduction in transmittance of PLA70/ID20 could ascribe to the PLA and PBAT co-continuous morphology in the film.

Discussion and Proposed Mechanism. Given the observed improvements in the mechanical properties and transmittance of PLA70/ID20, it is important to consider what mechanisms underpin these changes.

The elevated T_g of irradiated PLA/PBAT/CaCO₃ films indicates that PLA was cross-linked after UV exposure. The proposed photo crosslinking mechanism of PLA in PLA/PBAT/CaCO₃ films is shown in Figure 7. As shown, UV irradiation may generate tertiary (A) and primary (B) radicals from PLA main chains by the hydrogen abstraction of the excited triplet BP under UV irradiation.

The recombination of the tertiary and primary radicals forms the covalent crosslinking between PLA chains. In addition, GMA and TAIC are also involved in the photo-crosslinking of PLA.

Of course, the above reactions can occur both in the amorphous region of PLA and in the crystalline region. But the effect of UV irradiation on PLA50 with PBAT continuous phase was not significant compared to that on PLA100, which indicates that the degradation and cross-linking of PBAT caused by UV irradiation was insignificant in PLA50.

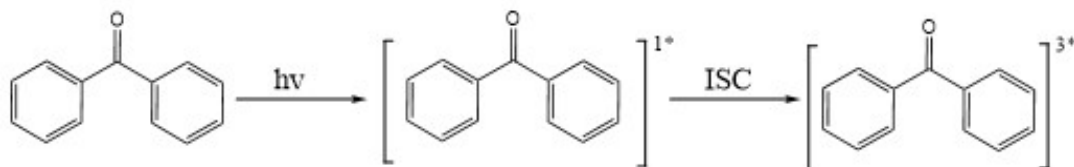


Figure 7: (1) BP photo excitation

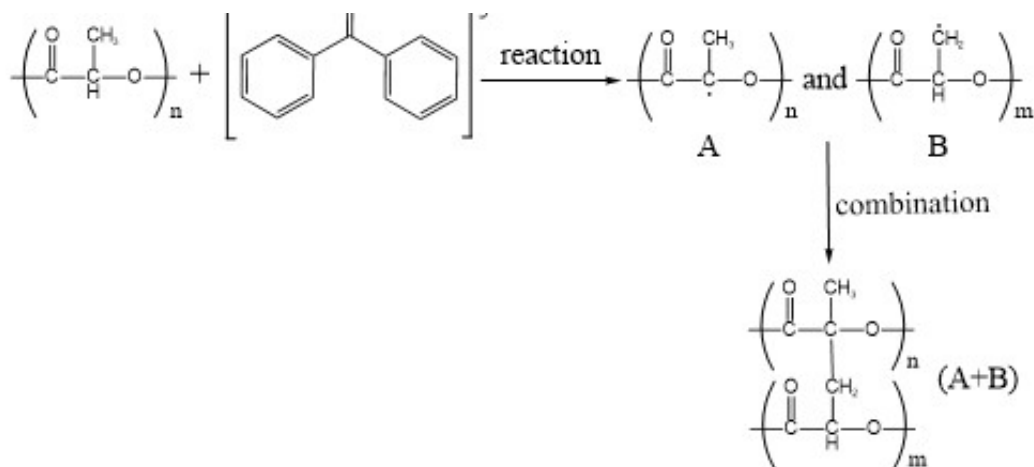


Figure 7: (2) PLA photo crosslinking

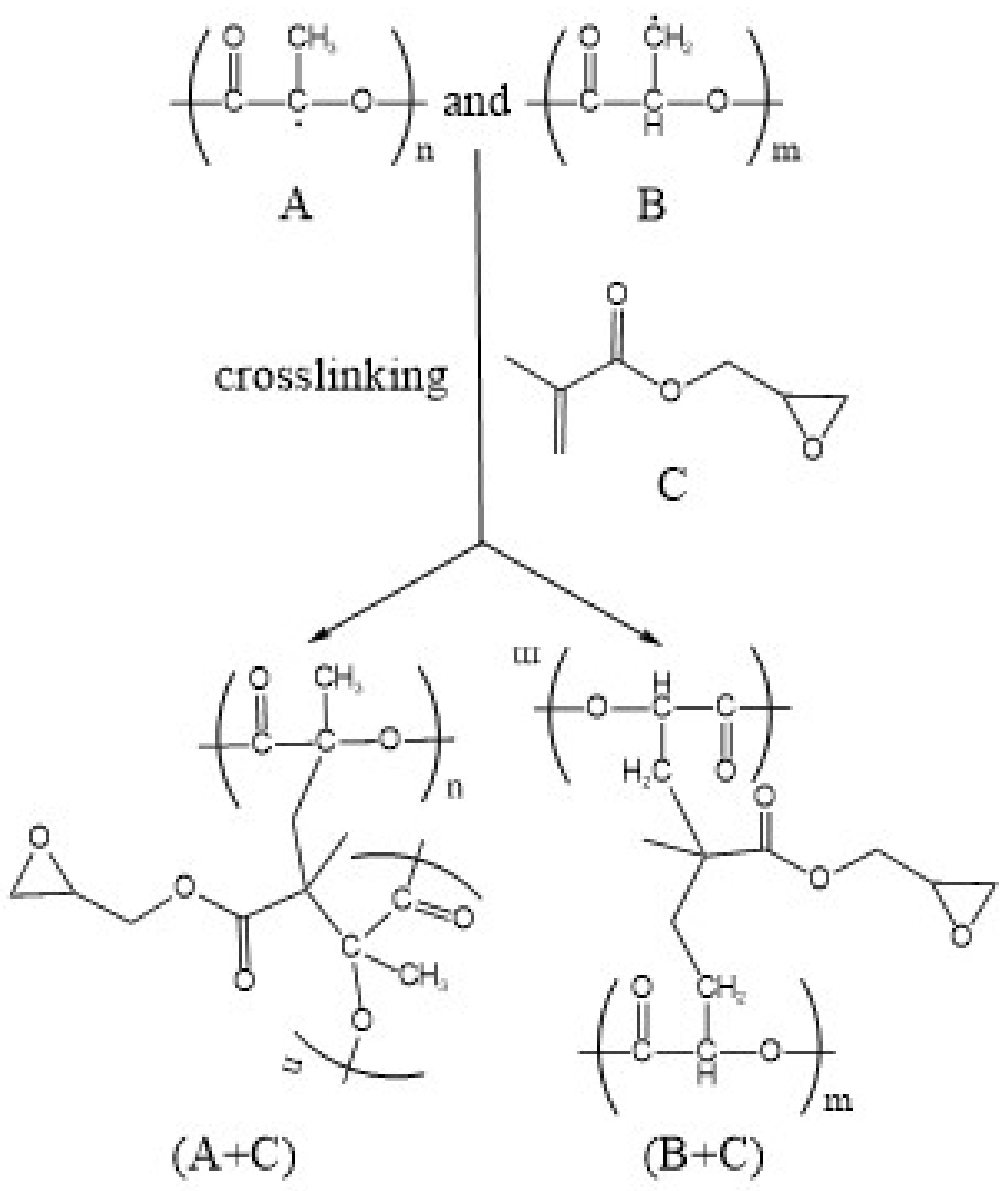


Figure 7: (3) GMA involved in PLA photo crosslinking

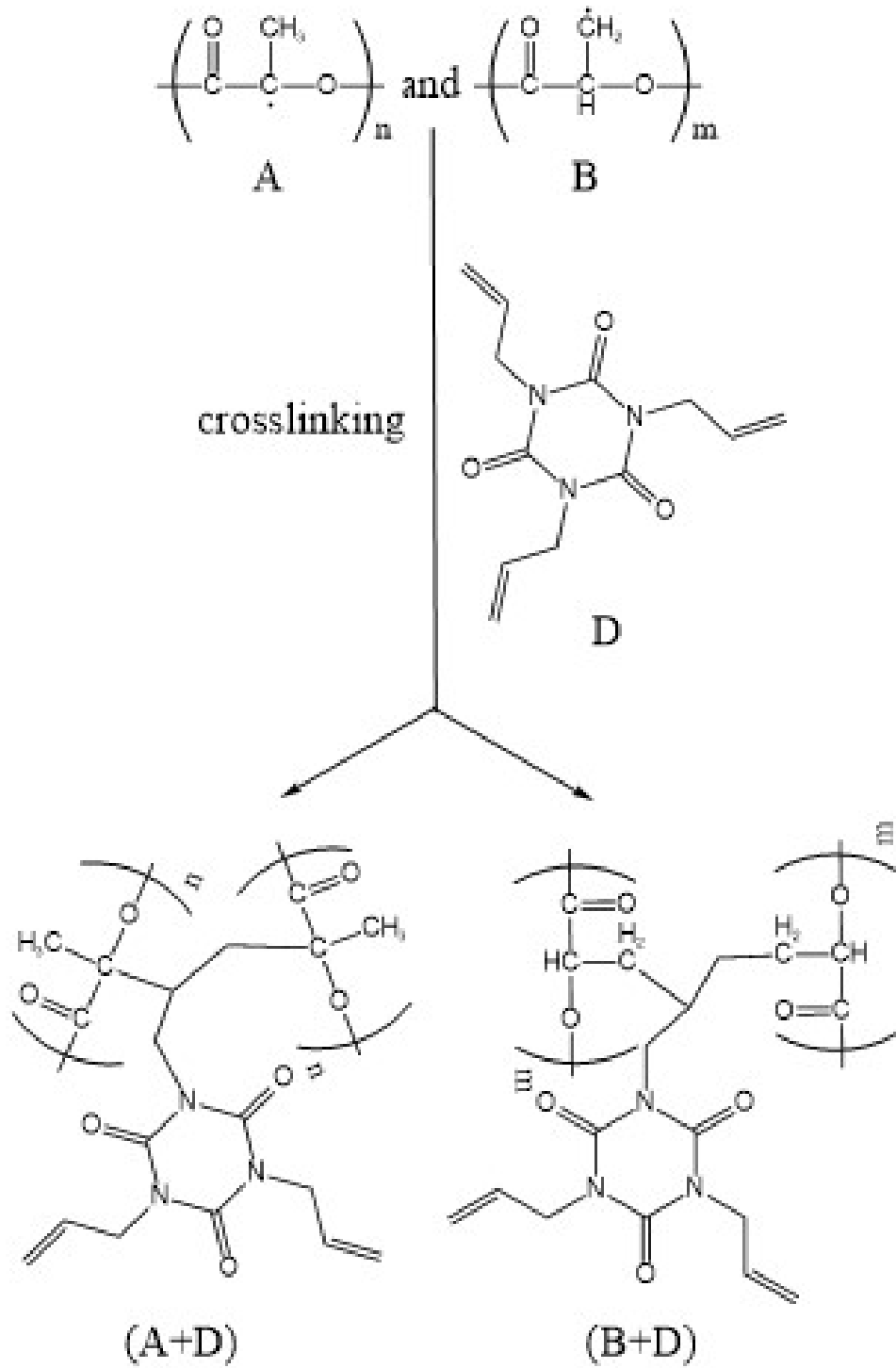


Figure 7: (4) TAIC involved in PLA photo crosslinking (5) GMA and TAIC involved in PLA photo crosslinking

The photo crosslinking of PLA involving GMA and TAIC can be considered as (A+C+D), (B+C+D), and (A+B+C+D).

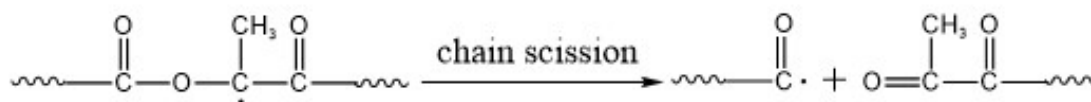


Figure 7: (6) PLA chain scission

Figure 7: The proposed photo crosslinking mechanism of PLA in PLA/PBAT/CaCO₃ films with the presence of GMA, TAIC and BP.

Conclusion

The UV radiation developed in this study was found to be a simple and cost-effective way for the modification of PLA70 with PLA and PBAT co-continuous phases. UV irradiation simultaneously increased the tensile strength and fracture energy of PLA70. Of course, this method needs to be within the moderate irradiation dose range, i.e., 20 J/cm², and higher than the dose limit is still harmful to the mechanical property of PLA70. In addition, this method is not suitable for PLA50, i.e. complexes of PLA/PBAT/CaCO₃ where PBAT is a mono-continuous phase. Contrastingly, UV irradiation increased the tensile strength and decrease the fracture energy of PLA100, but simultaneously decrease the tensile strength and fracture energy of PLA50. In addition, UV irradiation improved the transparency of PLA70, while decreasing the transparency of PLA100 and PLA50.

The different effects of UV radiation on the performance of PLA100, PLA70 and PLA50 are attributed to the differences in the continuous phases in the PLA/PBAT/CaCO₃ complexes. The contact surface between the two phases in the co-continuous phase is large, and UV irradiation can enhance the interconnection at the interface.

The glass transition temperature of PLA100 increased after UV exposure, but the T_g of PLA70 and PLA50 unchanged or varied within the error range. The crystallization temperature did not change after UV exposure, but the crystallizability significantly decreased. This indicates that the cross-linking caused by UV irradiation occurs not only in the amorphous region of PLA, but also in its crystalline region. Cross-linking restricts the movement of PLA molecular chains and reduces their crystallization ability.

Author contribution

The authors declare no competing financial interest.

Acknowledgments

This study was supported by the Innovation Fund of Henan Hairuixiang Technology Co., Ltd (Grant 2021001).

References

1. Muneer F, Habibullah N, Amna A, Warda Z (2021). Bioplastics from Biopolymers: An Eco-Friendly and Sustainable Solution of Plastic Pollution. *Polym. Sci. Ser 63*: 47-63.
2. Tyagi P, Agate S, Velev OD, Lucia L, Pal L (2022). A critical review of the performance and soil biodegradability profiles of biobased natural and chemically synthesized polymers in industrial applications. *Environ Sci Technol* 56: 2071-95.
3. Milovanovic S, Pajnik J, Lukic I (2022). Tailoring of advanced poly(lactic acid)-based materials: A review. *J. Appl Polym Sci* 139, e51839.
4. Rosa JC, Bonvent JJ, Santos AR (2022). Poly(epsilon-caprolactone)/Poly(lactic acid) fibers produced by rotary jet spinning for skin dressing with antimicrobial activity. *Journal of biomaterials applications* 36, 1641-51.
5. Mulla MZ, Rahman M, Marcos B, Tiwari B, Pathania S (2021). Poly Lactic Acid (PLA) Nanocomposites: Effect of Inorganic Nanoparticles Reinforcement on Its Performance and Food Packaging Applications. *Molecules* 26: 1967.
6. Wang K, Sun X, Long B, Li F, Yang C (2021). Green production of biodegradable mulch films for effective weed control. *ACS Omega* 6: 32327-33.
7. Caronna F, Glimpel N, Paar GP, Gries T, Blaeser A (2022). Manufacturing, characterization, and degradation of a poly(lactic acid) warp-knitted spacer fabric scaffold as a candidate for tissue engineering applications. *Biomater. Sci.*10: 3793-807.
8. Zhang M, Jiang C, Wu Q, Zhang G, Liang F (2022). Poly(lactic acid)/poly(butylene succinate) (PLA/PBS) layered composite gas barrier membranes by anisotropic janus nanosheets compatibilizers. *ACS Macro Lett* 11: 657-62.
9. Sun Y, Wang X, Xia S, Zhao J Cu(II) (2022). adsorption on poly(lactic acid) microplastics: Significance of microbial colonization and degradation. *Chem. Eng. J* 429: 132306.
10. Razavi M, Wang SQ (2019). Why Is Crystalline Poly(lactic acid) Brittle at Room Temperature? . *Macromolecules* 52: 5429-41.
11. Jia S, Zhao L, Wang X, Chen Y, Pan H. (2022). Poly (lactic acid) blends with excellent low temperature toughness: A comparative study on poly (lactic acid) blends with different toughening agents. *International Journal of Biological Macromolecules* 201: 662-75.
12. Jacek A, Michał N (2021). Development of toughened flax fiber reinforced composites. Modification of Poly(lactic acid)/Poly(butylene adipate-co-terephthalate) Blends by Reactive Extrusion Process. *Materials* 14: 1523
13. Deng Y, Yu C, Wongwiwattana P, Thomas NL (2018). Optimising ductility of poly (Lactic Acid)/Poly (Butylene Adipate-co-Terephthalate) blends through co-continuous phase morphology. *Journal of Polymers and the Environment* 26: 3802-16.
14. Naser A, Deiab I, Defersha F, Yang S (2021). Expanding poly(lactic acid) (PLA) and polyhydroxyalkanoates (PHAs) applications: A review on modifications and effects. *Polymers* 13: 4271.
15. Khosravi A, Fereidoon A, Khorasani MM, Naderi G, Ganjali MR, Zarrintaj P, Saeb MR, Gutierrez TJ (2020). Soft and hard sections from cellulose-reinforced poly(lactic acid)-based food packaging films: A critical review. *Food Packaging Shelf* 23: 100429.

16. Zhou L, Ke K, Yang MB, Yang W (2021). Recent progress on chemical modification of cellulose for high mechanical-performance Poly(lactic acid)/Cellulose composite: A review. *Compos. Commun* 23: 100548.
17. Deetuum C, Samthong C, Choksrivichit S, Somwangthanaroj A. (2020). Isothermal cold crystallization kinetics and properties of thermoformed poly (lactic acid) composites: effects of talc, calcium carbonate, cassava starch and silane coupling agents. *Iran. Polym. J.* 19: 103-16.
18. Meekum U, Kingchang P (2017). Peroxide/silane crosslinked poly(lactic acid) hybrid biocomposite reinforced with empty fruit bunch and cotton fibers for hot-fill food packaging. *Bioresources* 12: 5086-101.
19. Long C, Yang J, Ke W, Feng C, Qiang F (2010). Largely improved tensile extensibility of poly(L-lactic acid) by adding poly(ϵ -caprolactone). *Polym. Int* 59: 1154-61.
20. Zhang R, Cai C, Liu Q, Hu S (2017). Enhancing the melt strength of poly(lactic acid) via micro-crosslinking and blending with poly(butylene adipate-co-butylene terephthalate) for the preparation of foams. *J. Polym. Environ.* 25: 1335-41.
21. Tang H, Zhou L, Bian X, Wang T, Feng L, Zhang B, Liu Y, Chen X (2022). Highly toughened poly (lactic acid) blends plasticized by cardanol in presence of dicumyl peroxide. *Mater. Lett* 313: 131777.
22. Long Y, Toikka G, Dean K, Bateman S, Nguyen T. Foaming behaviour and cell structure of poly(lactic acid) after various modifications. *Polym. Int* 62: 759-65.
23. Tsuji H, Shimizu K, Sato Y (2012). Hydrolytic degradation of poly(L-lactic acid): Combined effects of UV treatment and crystallization. *J. Appl. Polym. Sci* 125: 2394-406.
24. Zhao X, Li J, Liu J, Zhou W, Peng S (2021). Recent progress of preparation of branched poly(lactic acid) and its application in the modification of polylactic acid materials. *International Journal of Biological Macromolecules* 193(Pt A), 874-92.
25. Wang X, Shi M, Zhou W, et al. (2019). Preparation and cross-linking behavior of active prepolymer of multiarm-poly(lactic acid). *Plastics (chinese)* 48: 101-4 +108.
26. Ren Z, Li H, Sun X, Yan S, Yang Y (2012). Fabrication of High Toughness Poly(lactic acid) by Combining Plasticization with Cross-linking Reaction. *Ind. Eng. Chem. Res* 51: 21, 7273-8.
27. Vidotto M, Mihaljevic B, Auhar G, Vidovi E, Vali S (2021). Effects of γ -radiation on structure and properties of poly(lactic acid) filaments. *Radiat. Phys. Chem* 184: 109456.
28. Lee JM, Hong JS, Ahn KH (2019). Particle percolation in a poly (lactic acid)/calcium carbonate nanocomposite with a small amount of a secondary phase and its influence on the mechanical properties. *Polym. Composite* 40: 4023-32.
29. Xia X, Shi X, Liu W, He S, Zhu C (2020). Liu H. Effects of gamma irradiation on properties of PLA/flax composites. *Iran. Polym. J* 29: 581.
30. Madera-Santana TJ, Melendez R, González-García G, Quintana-Owen P, Pillai SD (2016). Effect of gamma irradiation on physicochemical properties of commercial poly(lactic acid) clamshell for food packaging. *Radiat. Phys. Chem* 123: 6.
31. Iuliano A, Nowacka M, Rybak K, Rzepna M (2020). The effects of electron beam radiation on material properties and degradation of commercial PBAT/PLA blend. *J. Appl. Polym. Sci* 137: 48462.
32. Malinowski R, Moraczewski K, Raszowska-Kaczor A (2020). Studies on the uncrosslinked fraction of PLA/PBAT

blends modified by electron radiation. *Materials* 13: 1068.

33. Deng Y, Yu C, Wongwiwattana P, Thomas NL (2018). Optimising ductility of poly(Lactic Acid)/Poly(Butylene Adipate-co-Terephthalate) blends through co-continuous phase morphology. *J. Polym. Environ* 26: 3802-16.

34. Ke L, Peng J, Turng LS, Huang HX (2011). Dynamic rheological behavior and morphology of polylactide/poly(butylenes adipate-co-terephthalate) blends with various composition ratios. *Adv Polym. Technol.* 30: 150-7.

35. Zhao G, Thompson MR, Zhu Z (2019). Effect of poly(2-ethyl-2-oxazoline) and UV irradiation on the melt rheology and mechanical properties of poly(lactic acid) *J Appl Polym Sci* 136: 48023.

36. Koo G H, Jang J (2012). Preparation of melting-free poly(lactic acid) by amorphous and crystal crosslinking under UV irradiation. *J Appl Polym Sci* 38056.